

# Simulating prescribed particle densities in the grand canonical ensemble using iterative algorithms

Attila Malasics,<sup>1</sup> Dirk Gillespie,<sup>2</sup> and Dezső Boda<sup>1,2,a)</sup>

<sup>1</sup>Department of Physical Chemistry, University of Pannonia, P.O. Box 158, H-8201 Veszprém, Hungary

<sup>2</sup>Department of Molecular Biophysics and Physiology, Rush University Medical Center, Chicago, Illinois 60612, USA

(Received 30 November 2007; accepted 10 January 2008; published online 24 March 2008)

We present two efficient iterative Monte Carlo algorithms in the grand canonical ensemble with which the chemical potentials corresponding to prescribed (targeted) partial densities can be determined. The first algorithm works by always using the targeted densities in the  $kT \log(\rho_i)$  (ideal gas) terms and updating the excess chemical potentials from the previous iteration. The second algorithm extrapolates the chemical potentials in the next iteration from the results of the previous iteration using a first order series expansion of the densities. The coefficients of the series, the derivatives of the densities with respect to the chemical potentials, are obtained from the simulations by fluctuation formulas. The convergence of this procedure is shown for the examples of a homogeneous Lennard-Jones mixture and a NaCl–CaCl<sub>2</sub> electrolyte mixture in the primitive model. The methods are quite robust under the conditions investigated. The first algorithm is less sensitive to initial conditions. © 2008 American Institute of Physics. [DOI: 10.1063/1.2839302]

## I. INTRODUCTION

In the grand canonical (GC) ensemble the chemical potentials of the various species ( $\mu_i$ ) are fixed, while the number of particles of these species ( $N_i$ ) fluctuate around their average value ( $\bar{N}_i$ ), as determined by the chemical potentials, the temperature ( $T$ ), and system size (fixed by volume  $V$ ). Monte Carlo (MC) simulations realize statistical sampling in the GC ensemble by random insertion/deletion steps.<sup>1,2</sup> GCMC simulations have advantages in many applications. For example, in the GC ensemble it is straightforward to calculate entropic quantities such as free energy. Also, in the simulations of mixtures where a species is present in low quantity (e.g., physiological Ca<sup>2+</sup> concentrations of 10<sup>-6</sup>–10<sup>-3</sup> mol), the use of GC ensemble is crucial.<sup>3</sup>

In mixtures, the densities of the various species ( $\rho_i = \bar{N}_i/V$ ) are called partial densities in physical chemistry, while various definitions of concentrations are used in solution chemistry. These densities are outputs of the GCMC simulations. In many applications, however, the purpose is to perform simulations for prescribed (or targeted) densities ( $\rho_i^{\text{targ}}$ ) in the GC ensemble. For this purpose, one should know the chemical potentials that correspond to the targeted densities in advance. Finding these chemical potentials requires some additional work.

A straightforward solution from a thermodynamic point of view is to perform several simulations—in any ensemble—and to calculate the missing thermodynamic quantities from standard thermodynamic relations such as the Gibbs-Helmholtz equation.<sup>4</sup> This procedure, nevertheless, can be too cumbersome and time consuming—especially for mixtures. In the canonical and other (for example, in the

isothermal-isobaric) ensembles one can apply Widom's test particle method to calculate the chemical potentials.<sup>5</sup> Shing and Gubbins extended this method applying both particle insertions and particle deletions, arriving at a more accurate estimate of the chemical potential.<sup>6</sup> Their method is a special case of the overlapping distribution method of Bennett<sup>7</sup> to compute free energy differences.

If one wants to use the ensemble where particle insertions/deletions and so particle number fluctuations naturally occur, the GC ensemble should be used. In the GC ensemble, the trivial procedure is to perform multiple simulations and obtain chemical potentials by interpolation—also a cumbersome process in the case of mixtures.<sup>8</sup> Recently, Lamperski<sup>9</sup> proposed an elegant method to compute the activity coefficients in electrolytes of fixed concentrations using the GC ensemble. The method is called the inverse GCMC (IGCMC) method and it is based on adjusting the chemical potentials after blocks of the simulations on the basis of the densities obtained from the blocks. Thus, both the chemical potentials and the particle numbers are fluctuating quantities in the GCMC simulations, but they fluctuate around the desired values.

In this paper we propose two simple iterative GCMC algorithms that are easy to program, converge fast, and are robust under many conditions. The first method changes the value of the excess chemical potential in the iterations, while the second method extrapolates the chemical potentials using thermodynamic derivatives calculated from fluctuation formulas. The methods are introduced on the examples of two typical systems: (1) for a binary mixture of Lennard-Jones (LJ) particles at a high density above the critical temperature and (2) for a NaCl–CaCl<sub>2</sub> mixture described by the primitive model electrolytes. The methods are examined from the

<sup>a)</sup>Authors to whom correspondence should be addressed. Electronic addresses: boda@almos.vein.hu and dezso\_boda@rush.edu.

points of view of their sensitivity to starting conditions and how fast do they converge to the targeted state.

No long range corrections were used in either cases. The systems with cut-off potentials are just as well defined systems as those computed with long range contributions. Therefore, they can be used to test the efficiency of the proposed algorithms. Of course, the relationship between the densities and the chemical potentials given by the algorithms will be that of the system with cut-off potentials, but they are well-defined nevertheless. We have performed a system-size check and found that the width of the simulation cell, and thus long range corrections, have small effect on the chemical potential-density relations.

## II. ITERATING THE EXCESS CHEMICAL POTENTIAL

### A. Method

The total chemical potential can be written as

$$\mu_i^{\text{tot}} = kT \log(\Lambda_i^3) + \mu_i, \quad (1)$$

where  $\Lambda_i = h / (2\pi m_i kT)^{1/2}$  is the de Broglie wavelength,  $h$  is the Planck constant,  $m_i$  is the particle mass for species  $i$ , and  $k$  is the Boltzmann constant. The term  $\mu_i$  (without superscript) is the one used in MC simulations that sample only the configurational space; the  $kT \log(\Lambda_i^3)$  term drops out from the acceptance probability criterions of the insertion/deletion steps because it does not depend on the configurational coordinates. The quantity  $\mu_i$  is sometimes called the configurational chemical potential and can be decomposed as

$$\mu_i = kT \log(\rho_i) + \mu_i^{\text{ex}}, \quad (2)$$

where  $\mu_i^{\text{ex}}$  is the excess chemical potential. The term residual chemical potential is also used for this excess term. The value of  $\mu_i$  depends on the unit of length in the calculations [through the density, so it would be more appropriate to write the logarithmic term as  $\log(\rho_i/\rho_0)$ , where  $\rho_0$  is some fixed density unit].

The variables that are changing in our iteration process are the excess chemical potentials  $\mu_i^{\text{ex}}$ , while in the logarithmic (ideal gas) term we always use the targeted densities  $\rho_i^{\text{targ}}$ . The steps of the  $n$ th iteration are as follows:

- (1) Calculate  $\mu_i(n) = kT \log(\rho_i^{\text{targ}}) + \mu_i^{\text{ex}}(n)$  using the targeted densities of the individual components in the ideal gas term (the integer  $n$  in parentheses is the index of the iteration).
  - In the first iteration, we start with some reasonable guess for the values of  $\mu_i^{\text{ex}}(1)$  [sometimes even the ideal gas value  $\mu_i^{\text{ex}}(1) = 0$  is good enough].
  - In subsequent iterations, the values calculated from the previous iteration are used:  $\mu_i^{\text{ex}}(n) = \mu_i^{\text{ex}}(n-1)$  if  $n > 1$ .
- (2) Perform a GCMC simulation (an iteration) using these chemical potentials. The results of this simulation are the average densities  $\bar{\rho}_i(n)$  and the average excess chemical potentials are obtained as  $\bar{\mu}_i^{\text{ex}}(n) = \mu_i(n) - kT \log(\bar{\rho}_i(n))$ .

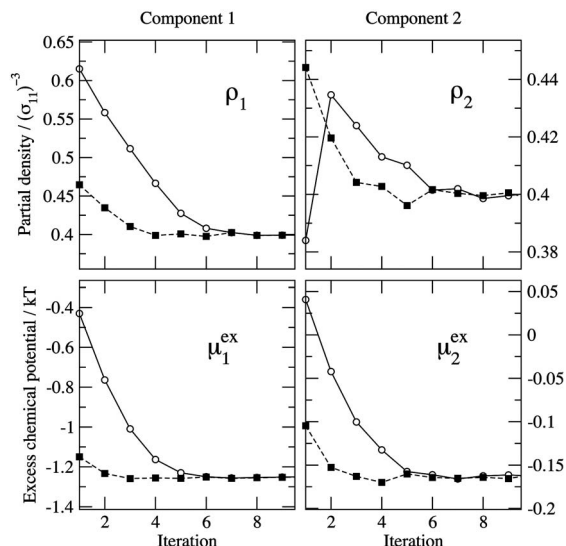


FIG. 1. Convergence of partial densities and excess chemical potentials for a LJ-mixture. Open circles with solid lines refer to the case when we start from the ideal gas condition [ $\mu_1^{\text{ex}}(1)/kT = \mu_2^{\text{ex}}(1)/kT = 0$ ], while full squares with dashed lines refer to the case when we start from the excess chemical potentials  $\mu_1^{\text{ex}}(1)/kT = -1$  and  $\mu_2^{\text{ex}}(1)/kT = 0$ .

- (3) Use these output excess chemical potentials of the iteration as the input chemical potentials of the next iteration,  $\mu_i^{\text{ex}}(n+1) = \bar{\mu}_i^{\text{ex}}(n)$ , and jump to step 1.

The advantage of this procedure is that an existing GCMC code can be used as the core of the algorithm, and the iteration as an outer loop is easily programmable.

### B. Results for a Lennard-Jones mixture

The LJ potential is given by

$$\phi_{\text{LJ}}(r_{ij}) = 4\varepsilon_{ij} \left[ \left( \frac{\sigma_{ij}}{r_{ij}} \right)^{12} - \left( \frac{\sigma_{ij}}{r_{ij}} \right)^6 \right], \quad (3)$$

where the  $i, j$  subscripts refer to species and  $r_{ij}$  is the distance of two molecules of species  $i$  and  $j$ . We have simulated a binary LJ mixture with the potential and distance parameters  $\varepsilon_{12} = 0.7071\varepsilon_{11}$ ,  $\varepsilon_{22} = 0.5\varepsilon_{11}$ ,  $\sigma_{12} = 0.75\sigma_{11}$ , and  $\sigma_{22} = 0.5\sigma_{11}$ . We used the reduced temperature  $kT/\varepsilon_{11} = 1.5$  that is above the critical temperature of the pure LJ fluid. A cubic simulation cell was used with a periodic boundary condition applying the minimum image convention. If we use the size parameter of species 1 ( $\sigma_{11}$ ) as the distance unit (reduced units), the targeted densities in our example are  $\rho_1^{\text{targ}}\sigma_{11}^3 = \rho_2^{\text{targ}}\sigma_{11}^3 = 0.4$ . The average number of particles in the simulation was about 400 (200 for each species).

First, we started the iteration process with the ideal gas values for the excess chemical potentials:  $\mu_1^{\text{ex}}(1)/kT = \mu_2^{\text{ex}}(1)/kT = 0$ . The iteration finds the correct values relatively quickly and after five to six iterations it only refines the answer (Fig. 1, open circles). We find that relatively short simulations are able to drive the system very close to the targeted values. Long simulations per iteration are necessary if one wants to obtain accurate values at the end of the iteration process. Thus, it is a good idea to increase the length of the simulations gradually during the iteration process. In

these calculations, we started the iteration process with 100 MC cycles and finished with 5000 MC cycles in the tenth iteration. In an MC cycle 6000 attempts were made to perform an MC move. 60% of the MC moves was particle insertion/deletion, while in the remaining 40% of the usual particle displacements were performed. Insertion/deletion and displacement of the larger particle were attempted more frequently because the acceptance ratio for this species was smaller. We intentionally ran short simulations to test the efficiency of the iteration process. We found that relatively short simulations are sufficient, but this depends (1) on the system under consideration and (2) on the needs of the simulator for the accuracy of the final result. Thus, these details will have to be sorted out by the user of the method, so we do not discuss the lengths of the iterations in this paper any further.

The process is not very sensitive to the guess for the initial values of the excess chemical potentials. For example, we started an iteration with  $\mu_{\text{NaCl}}^{\text{ex}}(1)/kT = -1$  and  $\mu_{\text{CaCl}_2}^{\text{ex}}(1)/kT = 0$  (Fig. 1, solid squares). The convergence is faster because this guess is closer to the final results  $\mu_{\text{NaCl}}^{\text{ex}}(1)/kT = -1.25$  and  $\mu_{\text{CaCl}_2}^{\text{ex}}(1)/kT = -0.16$ . Because the first iterations are relatively short, this does not influence the length of the whole iteration process considerably. It is the refinement of the final answer which is more time consuming.

Finding a good initial guess is more important when the temperature is lower than the critical temperature. In this case, the system tends to fluctuate between the vapor and liquid phases because an iteration might get into the metastable region. This means that the algorithm is not as robust in the liquid phase under the critical temperature (in the vapor phase, it is more robust because the excess term is small compared to the ideal term). Here, the user should use the algorithm with extra care, just as the GCMC simulation method *in general* should be used with extra care in this regime. In this regime, the particle insertion method<sup>5</sup> applied in the canonical ensemble is more advantageous because the system is not allowed to change phase at fixed densities. Phase separation can occur, nevertheless, inside the simulation cell if we perform the simulation in the two-phase regime.

### C. Results for a primitive electrolyte mixture

Electrolytes are conventionally simulated in the GC ensemble by inserting/deleting neutral groups of ions,<sup>15</sup> usually  $\nu_+$  cations and  $\nu_-$  anions (where  $\nu_+$  and  $\nu_-$  are the stoichiometric coefficients). In this case, instead of the chemical potentials of the individual ions, the chemical potentials of the salts are used in the GCMC simulations. In the example shown here, we simulate a mixture of NaCl and CaCl<sub>2</sub>. The chemical potentials of the salts are

$$\mu_{\text{NaCl}} = \mu_{\text{Na}} + \mu_{\text{Cl}} = \log(\rho_{\text{Na}}\rho_{\text{Cl}}) + \mu_{\text{NaCl}}^{\text{ex}}, \quad (4)$$

$$\mu_{\text{CaCl}_2} = \mu_{\text{Ca}} + 2\mu_{\text{Cl}} = \log(\rho_{\text{Ca}}\rho_{\text{Cl}}^2) + \mu_{\text{CaCl}_2}^{\text{ex}}, \quad (5)$$

where the salt excess chemical potentials are

$$\mu_{\text{NaCl}}^{\text{ex}} = \mu_{\text{Na}}^{\text{ex}} + \mu_{\text{Cl}}^{\text{ex}}, \quad (6)$$

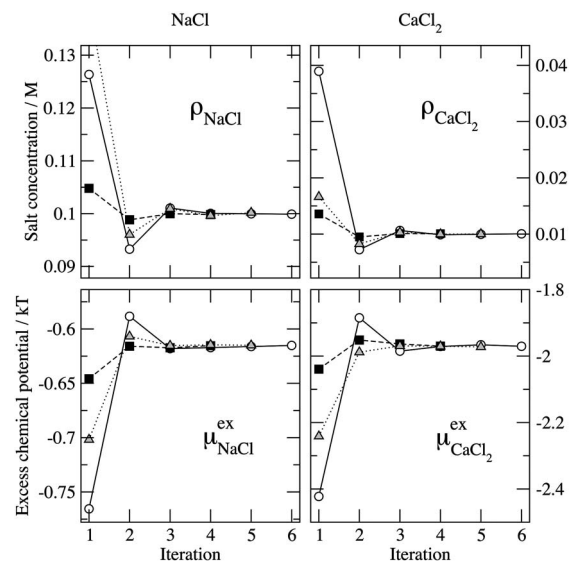


FIG. 2. Convergence of salt concentrations and excess chemical potentials for a NaCl–CaCl<sub>2</sub> electrolyte mixture. Open circles with solid lines refer to the case when we start from the ideal gas condition [ $\mu_{\text{NaCl}}^{\text{ex}}(1)/kT = \mu_{\text{CaCl}_2}^{\text{ex}}(1)/kT = 0$ ]; gray triangles with dotted lines refer to the case when we start from the condition [ $\mu_{\text{NaCl}}^{\text{ex}}(1)/kT = 0$  and  $\mu_{\text{CaCl}_2}^{\text{ex}}(1)/kT = -1$ ], while full squares with dashed lines refer to the case when we start from the MSA results [ $\mu_{\text{NaCl}}^{\text{ex}}(1)/kT = -0.504$  and  $\mu_{\text{CaCl}_2}^{\text{ex}}(1)/kT = -1.543$ ].

$$\mu_{\text{CaCl}_2}^{\text{ex}} = \mu_{\text{Ca}}^{\text{ex}} + 2\mu_{\text{Cl}}^{\text{ex}}. \quad (7)$$

The formalism can be readily extended to mixtures of any salts.

The ions are modeled as charged hard spheres immersed in a continuum dielectric ( $\epsilon = 80$ ) at temperature  $T = 300$  K and so have an interaction potential (in Gauss units) of

$$\phi(r_{ij}) = \frac{z_i z_j e^2}{\epsilon r_{ij}}, \quad (8)$$

for  $r_{ij} > R_i + R_j$  and infinite otherwise because the overlap of spheres is forbidden. In this equation,  $z_i$  and  $R_i$  are the valence and radius of ionic species  $i$ . In our example, Pauling radii are used for the radii of the ions: 0.95, 0.99, and 1.81 Å for Na<sup>+</sup>, Ca<sup>2+</sup>, and Cl<sup>-</sup>, respectively. The targeted salt concentrations are  $\rho_{\text{NaCl}} = 0.1$  mol and  $\rho_{\text{CaCl}_2} = 0.01$  mol. Our system size corresponds to targeted ion numbers of 200, 20, and 240 for Na<sup>+</sup>, Ca<sup>2+</sup>, and Cl<sup>-</sup>, respectively. The processes were started with 200 MC cycles with increasing lengths in later iterations.

We show iteration results for three initial guesses: (a) starting with the ideal gas conditions in the first iteration with  $\mu_{\text{NaCl}}^{\text{ex}}(1)/kT = \mu_{\text{CaCl}_2}^{\text{ex}}(1)/kT = 0$  (Fig. 2, open circles), (b) starting with the guess  $\mu_{\text{NaCl}}^{\text{ex}}(1)/kT = 0$  and  $\mu_{\text{CaCl}_2}^{\text{ex}}(1)/kT = -1$  in the first iteration (Fig. 2, gray triangles), and (c) starting with excess chemical potential values provided by the mean spherical approximation (MSA) in the first iteration with  $\mu_{\text{NaCl}}^{\text{ex}}(1)/kT = -0.603$  and  $\mu_{\text{CaCl}_2}^{\text{ex}}(1)/kT = -1.861$  (Fig. 2, full squares).

The situation is very similar to that observed in the case of the LJ mixture. Both the densities and the excess chemical potentials converge to the final values quite fast. The process converges faster if we start the iteration from something that

is closer to the final solution. The final excess chemical potentials are  $\mu_{\text{NaCl}}^{\text{ex}}/kT = -0.613$  and  $\mu_{\text{CaCl}_2}^{\text{ex}}/kT = -1.970$ .

We presented results for the chemical potentials of the salts (that correspond to the mean activity coefficients) in this work. The method, nonetheless, can be used to determine the individual chemical potentials (or the individual activity coefficients) of the ions. Our simulations gave results (not shown) for the individual chemical potentials that are consistent with the results for the salt chemical potentials. Because the main purpose of this paper is to present the algorithm, we do not pursue this question here. Computation of the chemical potentials of the individual ions is far from being trivial because of the problems with breaking charge neutrality when we insert an individual ion. Sloth and Sørensen applied the Widom particle insertion method to simulate the individual activity coefficients.<sup>10–12</sup> Modifications of the method by a neutralization of the charge of the test-particle have been proposed to overcome the strong system-size dependence of the results.<sup>13,14</sup> The IGCMC method of Lamperski<sup>9</sup> was shown to be able to reproduce the individual activity coefficients. Lamperski gives an analysis on the system size dependence of the individual and mean activity coefficients. We will report our results on this issue in a future paper.

The algorithm seems to be quite insensitive to the model studied. It is equally efficient for two very different systems such as electrolytes and the LJ fluid. Therefore, the efficiency of the algorithm is not affected by taking into account small energy terms such as the long-range corrections.

### III. EXTRAPOLATING THE CHEMICAL POTENTIAL

#### A. Method

The second method iterates the configurational chemical potentials instead of the excess ones. It is based on the first order series expansion of the densities. For a binary mixture,

$$\begin{aligned} \rho_1(n+1) &= \bar{\rho}_1(n) + \left( \frac{\partial \rho_1}{\partial \mu_1} \right) [\mu_1(n+1) - \mu_1(n)] \\ &\quad + \left( \frac{\partial \rho_1}{\partial \mu_2} \right) [\mu_2(n+1) - \mu_2(n)], \\ \rho_2(n+1) &= \bar{\rho}_2(n) + \left( \frac{\partial \rho_2}{\partial \mu_1} \right) [\mu_1(n+1) - \mu_1(n)] \\ &\quad + \left( \frac{\partial \rho_2}{\partial \mu_2} \right) [\mu_2(n+1) - \mu_2(n)]. \end{aligned} \quad (9)$$

The derivatives are taken by keeping  $T$ ,  $V$ , and the chemical potentials of the other species constant. If we prescribe that the densities in the next iteration should be the targeted densities [substitute  $\rho_i(n+1) = \rho_i^{\text{targ}}$  on the left-hand side of Eqs. (9)] then the chemical potentials in the next iteration  $\mu_1(n+1)$  and  $\mu_2(n+1)$  can be calculated from this system of linear equations (which can be straightforwardly extended to more than two components). Every other quantity in these equations are provided by the simulation of the  $n$ th iteration: the chemical potentials used in this iteration  $\mu_1(n)$  and  $\mu_2(n)$ , the partial densities provided by the simulation as

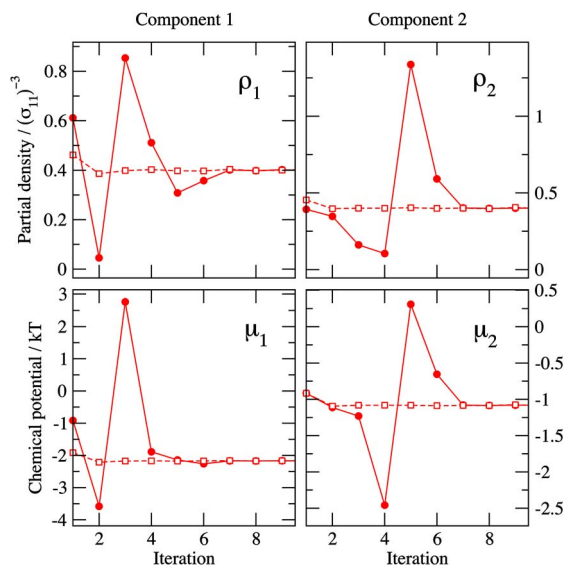


FIG. 3. (Color online) Convergence of partial densities and configurational chemical potentials for a LJ-mixture using the extrapolation method. Full circles with solid lines are obtained from the ideal gas starting condition  $\mu_1^{\text{ex}}(1)/kT=0$  and  $\mu_2^{\text{ex}}(1)/kT=0$ , while open squares with dashed lines are obtained with the starting condition  $\mu_1^{\text{ex}}(1)/kT=-1$  and  $\mu_2^{\text{ex}}(1)/kT=0$ .

ensemble averages  $\bar{\rho}_1(n)$  and  $\bar{\rho}_2(n)$ , and the thermodynamic derivatives as fluctuation formulas:

$$\left( \frac{\partial \rho_i}{\partial \mu_j} \right) = \frac{1}{kTV} (\overline{N_i N_j} - \bar{N}_i \cdot \bar{N}_j). \quad (10)$$

The fluctuation formulas are more poorly converging quantities in a simulation than the usual ensemble averages. The convergence of the above algorithm, nevertheless, does not require very accurate values for them. Even approximately accurate values of the derivatives drive the iteration closer to the desired state. Longer simulations, nevertheless, provide more accurate values for the densities and the fluctuation formulas, consequently, more accurate results at the end of the iteration process can be achieved.

#### B. Results for a Lennard-Jones mixture

We illustrate the method on the example of the LJ mixture used at the previous method. Because we need a relatively accurate value of the derivatives in this technique, we use the same length of simulations in every iteration. In the following figures, we plot the configurational chemical potentials because this is the quantity that we change by extrapolation in this technique.

Figure 3 shows the convergence of this method when starting from two different initial conditions (this figure corresponds to Fig. 1 at the previous method). In these simulations, 2000 MC cycles were used in every iteration. When we start the iteration from an initial condition with a state that is relatively close to the final state  $\mu_1^{\text{ex}}(1)/kT = -1$  and  $\mu_2^{\text{ex}}(1)/kT = 0$  (Fig. 3, open squares), the iteration is much faster than starting with the ideal gas condition (Fig. 3, full circles). In the latter case, the system is wandering about on the  $\{\rho_1(\mu_1, \mu_2), \rho_2(\mu_1, \mu_2)\}$  surfaces without any sign of convergence. When, nevertheless, it hits a state that is sufficiently close to the final state, it starts to converge fast. Be-

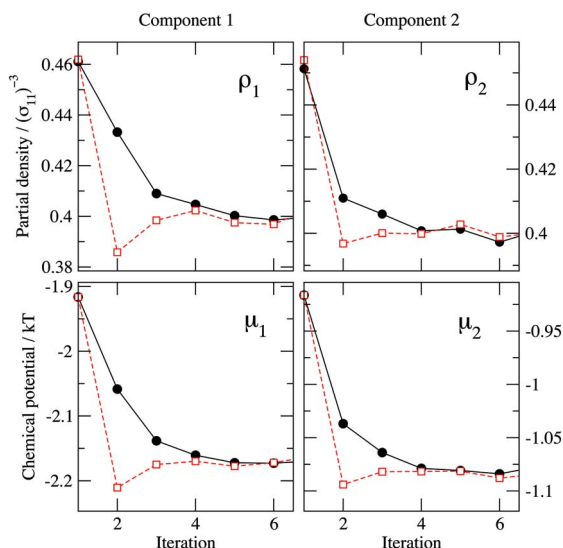


FIG. 4. (Color online) Convergence of partial densities and configurational chemical potentials for a LJ-mixture using the starting condition  $\mu_1^{\text{ex}}(1)/kT=-1$  and  $\mu_2^{\text{ex}}(1)/kT=0$ . Full circles with solid lines (black) are obtained with the method iterating the excess chemical potential, while open squares with dashed lines (red) are obtained with the extrapolation method.

cause the  $\rho_i(\mu_1, \mu_2)$  functions are monotonic at the supercritical temperature used in this study, the method finds the region of convergence sooner or later. It means that this extrapolation technique is more sensitive to initial conditions than the first method (compare Figs. 1 and 3).

Figure 4 shows a comparison between the convergences of the two methods. The same starting conditions [ $\mu_1^{\text{ex}}(1)/kT=-1$  and  $\mu_2^{\text{ex}}(1)/kT=0$ ] were used. The extrapolation method shows a fluctuation behavior in the first iterations, but after that it converges fast. The convergence of the first method is more stable. Not only the densities and the chemical potentials converge to the well defined values in the targeted state but also the thermodynamic derivatives. Figure 5 shows their convergence.

#### IV. SUMMARY

Two iterative algorithms have been proposed to determine the chemical potentials of mixtures with a prescribed

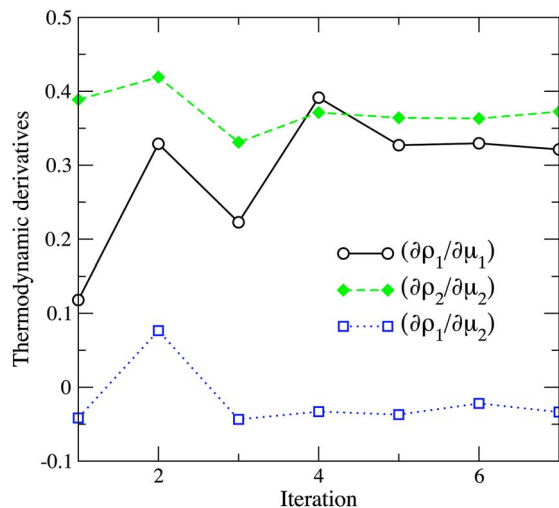


FIG. 5. (Color online) Convergence of the thermodynamic derivatives used in Eq. (9) as calculated from fluctuation formulas of Eq. (10).

composition. The idea of the first algorithm is that by using the targeted densities in the  $\log(\rho_i)$  terms and updating the excess chemical potentials in the iteration process, we automatically drive the system towards the desired conditions. The process converges fast, needing just a few iterations. Accuracy can be obtained by running longer simulations in later iteration steps.

The second method utilizes the capability of MC simulations to calculate the thermodynamic derivatives  $\partial \rho_i / \partial \mu_j$  as fluctuation formulas. Then, we can extrapolate the chemical potential in the  $(n+1)$ th iteration using the results of the  $n$ th iteration on the basis of a first order series expansion.

The first process seems to be more insensitive to starting conditions, at least above the critical point or at low densities. Establishing the limits of the method at high densities below the critical point—and where liquid-liquid immiscibility can occur—requires more careful analysis that will be published later. In the last months, we have used the first method extensively to compute the chemical potentials in various electrolyte mixtures.<sup>16–18</sup> Our experiences are very positive with the method. It works robustly practically for any composition even for tertiary mixtures.

The second algorithm is more sensitive to starting conditions. It converges fast and steadily once the process is close to the final value. Therefore, a combination of the two methods seems worthwhile: Start with the first method to drive the system close to its final state, then refine the answer with the second method and longer simulations.

The iteration is stopped by the potential users when the accuracy reached a certain limit, which depends on the user's needs. A natural choice for the criteria for when to stop the iteration is that when the difference between the chemical potentials and/or densities in two consecutive iterations is smaller than a chosen tolerance.

The usual difficulties characteristic to the GCMC method at high densities (where particle insertion is problematic) are inherent in this algorithm. These issues can be addressed by special sampling techniques (e.g., the cavity biased sampling<sup>19</sup>). Certainly, this algorithm is as good as the “mother algorithm,” the GCMC simulation technique, so any advanced sampling trick—that are available for many types of difficult situations in the literature—will also improve the efficiency of this algorithm.

The algorithm is presented for the examples of homogeneous systems simulated in cubic simulation cells with periodic boundary conditions. The method, nevertheless, is not restricted to such systems. It can also be used for inhomogeneous fluids where a part of the system, far from walls and other inhomogeneities, forms a homogeneous, bulk subsystem. Using the densities obtained for this bulk subsystem, the first algorithm also works as we successfully tested on our biological ion channels<sup>3</sup> (results not shown). In the case of the homogeneous system, however, the definition of the output densities (and thus, of the excess chemical potentials) is unambiguous as opposed to the inhomogeneous case where these densities are bound to the choice of the bulk subsystem.

## ACKNOWLEDGMENTS

The authors acknowledge the support of the Hungarian National Research Fund (OTKAK63322) and NIH Grant No. GM067241. We are grateful to Bob Eisenberg for the inspiring discussions and for providing the facilities to do this work. We are also grateful to Mónika Valiskó for all her support.

<sup>1</sup>G. E. Norman and V. S. Filinov, *High Temp.* **7**, 216 (1969).

<sup>2</sup>D. J. Adams, *Mol. Phys.* **28**, 1241 (1974); **29**, 307 (1975).

<sup>3</sup>D. Boda, M. Valiskó, B. Eisenberg, W. Nonner, D. Henderson, and D. Gillespie, *J. Chem. Phys.* **125**, 034901 (2006).

<sup>4</sup>M. P. Allen and D. J. Tildesley, *Computer Simulation of Liquids* (Clarendon, Oxford, 1987), pp. 49 and 50.

<sup>5</sup>B. Widom, *J. Chem. Phys.* **39**, 2808 (1969).

<sup>6</sup>K. S. Shing and K. E. Gubbins, *Mol. Phys.* **49**, 1121 (1983).

<sup>7</sup>C. H. Bennett, *J. Comput. Phys.* **22**, 245 (1976).

<sup>8</sup>A. Vitalis, N. A. Baker, and J. A. McCammon, *Mol. Simul.* **30**, 45 (2004).

<sup>9</sup>S. Lamperski, *Mol. Simul.* **33**, 1193 (2007).

<sup>10</sup>P. Sloth and T. S. Sørensen, *Chem. Phys. Lett.* **143**, 140 (1988).

<sup>11</sup>P. Sloth and T. S. Sørensen, *Chem. Phys. Lett.* **146**, 452 (1988).

<sup>12</sup>T. S. Sørensen, J. B. Jensen, and P. Sloth, *J. Chem. Soc., Faraday Trans.* **85**, 2649 (1989).

<sup>13</sup>B. R. Svensson and C. E. Woodward, *Mol. Phys.* **64**, 247 (1988).

<sup>14</sup>P. Sloth and T. S. Sørensen, *Chem. Phys. Lett.* **173**, 51 (1990).

<sup>15</sup>J. P. Valleau and L. K. Cohen, *J. Chem. Phys.* **72**, 5935 (1980).

<sup>16</sup>D. Boda, W. Nonner, M. Valiskó, D. Henderson, B. Eisenberg, and G. Gillespie, *Biophys. J.* **93**, 1960 (2007).

<sup>17</sup>D. Gillespie and D. Boda, "The anomalous mole fraction effect in calcium channels: A measure of preferential selectivity," *Biophys. J.* (submitted).

<sup>18</sup>D. Gillespie, D. Boda, Y. He, P. Apel, and Z. S. Siwy, "Synthetic nanopores as a test case for ion channel theories: The anomalous mole fraction effect," *Biophys. J.* (submitted).

<sup>19</sup>M. Mezei, *Mol. Phys.* **40**, 901 (1980); **61**, 565 (1987); **67**, 1207 (1989).